NUMERICAL ASSESSMENT OF A SPACE-CONSTRAINED VENTING SYSTEM WITH MULTI-CHAMBER PLUG MUFFLERS BY GA METHOD

Chiu Min-Chie
Department of Automatic Control Engineering, Chungchou Institute of Technology 6, Lane 2, Sec. 3, Shanchiao Rd., Yuanlin, Changhua 51003, Taiwan, R.O.C, minchie.chiu@msa.hinet.net

Chang Ying-Chun
Department of Mechanical Engineering, Tatung University, Taipei, Taiwan, R.O.C.

NUMERICAL ASSESSMENT OF A SPACE-CONSTRAINED VENTING SYSTEM WITH MULTI-CHAMBER PLUG MUFFLERS BY GA METHOD

Acknowledgements

NUMERICAL ASSESSMENT OF A SPACE-CONSTRAINED VENTING SYSTEM WITH MULTI-CHAMBER PLUG MUFFLERS BY GA METHOD

Min-Chie Chiu* and Ying-Chun Chang**

ABSTRACT

Recently, research on new techniques of single-chamber plug silencers has been addressed. However, the assessment of a multi-chamber plug muffler's optimal shape design within a constrained space as well as a pressure-drop limit which are mostly concerned with the necessity of operation and system venting in practical engineering work was rarely tackled. Therefore, this paper will not only analyze the sound transmission loss (*STL*) of a space-constrained multi-chamber plug muffler but also optimize the best design shape under a specified pressure drop.

In this paper, the generalized decoupling technique and plane wave theory used to solve the coupled acoustical problem of plug mufflers with perforated tubes are presented. The four-pole system matrix used to evaluate acoustic performance is also introduced in conjunction with a genetic algorithm (GA). Before the GA operation can be carried out, the accuracy of the mathematical model for a one-chamber plug muffler is checked using Munjal's experimental data.

To appreciate the sensitivity of a muffler's geometric parameters, the influence of sound transmission loss and related pressure drop with respect to design parameters is investigated. Furthermore, the noise reductions with respect to broadband exhaust noise emitted from a blower's inlet is also introduced and assessed. The optimal result in eliminating broadband noise reveals that the overall noise reductions with respect to various mufflers under a maximal allowable pressure drop of 800 (Pa) can achieve 40, 83 and 124 dB. Consequently, the

approach used for the optimal design of the multi-chamber plug mufflers under space and back pressure constrained conditions is indeed easy and quite effective.

I. INTRODUCTION

Because high noise levels cause psychological and physiological symptoms [1], the demand for low-noise levels of various products has become vital [9]. To overcome the low frequency noise emitted from a venting system, a reactive muffler is customarily used [10]. Moreover, because the constrained problem is mostly concerned with the necessity of operation and maintenance in practical engineering work, there is a growing need to optimize the acoustical performance within a confined space. In addition, in order to keep the volume-flow-rate steady in a venting system, the back pressure of mufflers within an allowable range is compulsory.

In the past decade, to increase acoustical performance, the assessment of new acoustical elements (internal perforated plug and non-plug tubes) was discussed by Sullivan and Crocker in 1978 [17]. Based on the coupled equations derived by Sullivan and Crocker, a series of theories and numerical techniques in decoupling the acoustical problems have been proposed [7, 15, 13, 18]. Concerning the flowing effect, Munjal [11] and Peat [14] published the generalized decoupling and numerical decoupling methods. Munjal *et al.* [12] investigated the acoustical effect and the system's back pressure with respect to several design parameters for perforated plug and cross-flow perforated mufflers without space constrained and back-pressure limited situation. However, the assessment of the muffler's optimal shape design within a constrained space and a back-pressure limit which are mostly concerned with the necessity of operation and system venting in practical engineering work was rarely tackled. In previous work, to solve the space-constraint problem, Yeh *et al.* [19, 20] and Chiu [4] developed the optimized shaped mufflers equipped with non-perforated ducts and by using numerical method. With the purpose of improving the acoustical performance, the shape optimizations of one-chamber mufflers in conjunction with perforated plug/non-plug and cross-flow tubes under

space-constrained situation were assessed [2, 3, 5]. However, the control of the system's back pressure which may retard the gas venting so as to damage the system had not been addressed.

In order to promote the acoustical performance and overcome the drawback of a possible overload pressure drop in the mufflers, three kinds of multi-chamber mufflers (a one-chamber, two-chamber, and a three-chamber plug muffler) equipped with plug perforated ducts under the fixed space volume and the specified allowable pressure drop is presented. To facilitate the numerical assessment, three different GA techniques (a tournament selection in elitism, a uniform crossover, and a randomized mutation) are adopted.

By adjusting the muffler's shape, increasing the chambers, and using the GA and numerical decoupling methods, the optimal acoustical performance of the mufflers with acceptable back pressure can be achieved.

II. MATHEMATICAL MODELS

In this paper, three kinds of multi-chamber plug mufflers (a one-chamber, two-chamber, and a three-chamber plug muffler) hybridized with perforated tubes were adopted for the noise abatement on the constrained blower room shown in Fig. 1. The outlines of these mufflers as noise-reduction devices are shown in Figs. 2(a), 2(b) and 2(c).

The acoustical fields with respect to various mufflers (a one-chamber, two-chamber, and a three-chamber plug muffler) are shown in Figs. 3(a), 3(b), and 3(c). As indicated in Figs. 2(a) and 3(a), the one-chamber plug muffler composed of four acoustical elements is identified with three categories of components — two straight ducts, one perforated expanded plug duct, and one perforated contracted plug duct. The related acoustic pressure p and acoustic particle velocity u within the muffler are represented by five nodes. As indicated in Figs. 2(b) and 3(b), the two-chamber plug muffler consisting of seven acoustical elements is also identified with three categories of components — three straight ducts, two perforated expanded plug ducts, and two perforated contracted plug ducts. The related acoustic pressure p and acoustic particle velocity u within the muffler are represented by eight nodes. Consequently, the three-chamber plug muffler shown in Figs. 2(c) and 3(c) is composed of ten acoustical elements and identified with three categories of components — four straight ducts, three perforated expanded plug ducts, and three perforated contracted plug ducts. Eleven nodes inside the acoustical elements represent the acoustical properties in the acoustical field with acoustic pressure p and acoustic particle velocity u at their due location. The detailed mathematical derivation of various muffler systems is presented below.

1. A One-Chamber Plug Muffler

As derived in the previous work [3], individual transfer matrixes with respect to straight ducts, expansion perforated ducts, and contracted perforated ducts are described as follows:
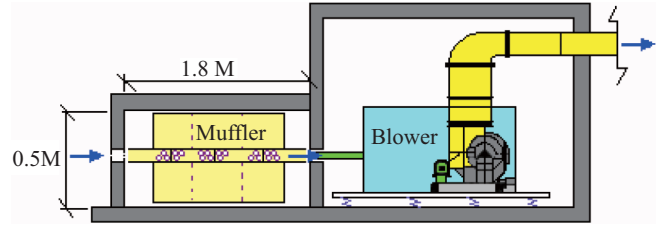

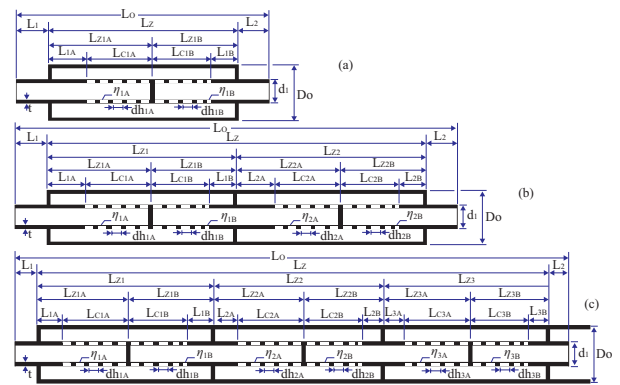Fig. 1. A multi-chamber plug muffler within a constrained blower room.

Fig. 2. The outlines of multi-chamber plug mufflers — (a) one-chamber, (b) two-chamber, and (c) three-chamber.
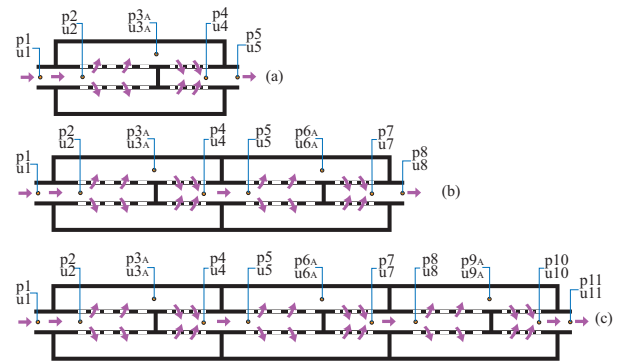

Fig. 3. The acoustical fields of multi-chamber plug mufflers (a) one-chamber, (b) two-chamber, and (c) three-chamber.

$$\begin{pmatrix} p_1 \\ \rho_o c_o u_1 \end{pmatrix} = e^{-jM_1 k(L_1 + L_{1A})/(1-M_1^2)} \begin{bmatrix} TS1_{1,1} & TS1_{1,2} \\ TS1_{2,1} & TS1_{2,2} \end{bmatrix} \begin{pmatrix} p_2 \\ \rho_o c_o u_2 \end{pmatrix} \quad (1)$$

$$\begin{pmatrix} p_2 \\ \rho_o c_o u_2 \end{pmatrix} = \begin{bmatrix} TPE2_{1,1} & TPE2_{1,2} \\ TPE2_{2,1} & TPE2_{2,2} \end{bmatrix} \begin{pmatrix} p_{3A} \\ \rho_o c_o u_{3A} \end{pmatrix} \quad (2)$$

$$\begin{pmatrix} p_{3A} \\ \rho_o c_o u_{3A} \end{pmatrix} = \begin{bmatrix} TPC3_{1,1} & TPC3_{1,2} \\ TPC3_{2,1} & TPC3_{2,2} \end{bmatrix} \begin{pmatrix} p_4 \\ \rho_o c_o u_4 \end{pmatrix} \quad (3)$$

$$\begin{pmatrix} p_4 \\ \rho_o c_o u_4 \end{pmatrix} = e^{-jM_3 k(L_2 + L_{1B})/(1-M_3^2)} \begin{bmatrix} TS4_{1,1} & TS4_{1,2} \\ TS4_{2,1} & TS4_{2,2} \end{bmatrix} \begin{pmatrix} p_5 \\ \rho_o c_o u_5 \end{pmatrix} \quad (4)$$

The total transfer matrix assembled by multiplication is

$$
\begin{pmatrix} p_1 \\ \rho_o c_o u_1 \end{pmatrix}
$$

$$
= e^{-jk\left[\frac{M_1(L_1+L_{1A})}{1-M_1^2}+\frac{M_4(L_2+L_{1B})}{1-M_4^2}\right]}
\begin{bmatrix} TS1_{1,1} & TS1_{1,2} \\ TS1_{2,1} & TS1_{2,2} \end{bmatrix}
\begin{bmatrix} TPE2_{1,1} & TPE2_{1,2} \\ TPE2_{2,1} & TPE2_{2,2} \end{bmatrix}
$$

$$
\begin{bmatrix} TPC3_{1,1} & TPC3_{1,2} \\ TPC3_{2,1} & TPC3_{2,2} \end{bmatrix}
\begin{bmatrix} TS4_{1,1} & TS4_{1,2} \\ TS4_{2,1} & TS4_{2,2} \end{bmatrix}
\begin{pmatrix} p_5 \\ \rho_o c_o u_5 \end{pmatrix}
\tag{5}
$$

A simplified form in a matrix is expressed as

$$
\begin{pmatrix} p_1 \\ \rho_o c_o u_1 \end{pmatrix}
=\begin{bmatrix} T_{11}^* & T_{12}^* \\ T_{21}^* & T_{22}^* \end{bmatrix}
\begin{pmatrix} p_5 \\ \rho_o c_o u_5 \end{pmatrix}
\tag{6}
$$

The sound transmission loss (*STL*) of a muffler is defined as [11]

$$
STL_1(Q, f, Aff_{11}, Aff_{12}, Aff_{13}, Aff_{14}, Aff_{15}, \eta_1, dh_1)
$$

$$
= 20\log\left(\frac{\left|T_{11}^* + T_{12}^* + T_{21}^* + T_{22}^*\right|}{2}\right) + 10\log\left(\frac{S_1}{S_4}\right)
\tag{7a}
$$

where

$$
Aff_{11} = L_Z / L_o; \; Aff_{12} = L_{Z1A} / L_Z; \; Aff_{13} = L_{C1A} / L_{Z1A};
$$

$$
Aff_{14} = L_{C1B}/L_{Z1B}; \; Aff_{15} = d_1/D_o; \; L_{Z1B} = L_Z - L_{Z1A};
$$

$$
L_{1A} = L_{Z1A} - L_{C1A}; \; L_{1B} = L_{Z1B} - L_{C1B}; \; L_1 = L_2 = (L_o - L_Z)/2
\tag{7b}
$$

The mean pressure drop (Δp_1) of a one-chamber plug muffler investigated by Munjal *et al.* [12] is

$$
\Delta p_1 = H_{1*}(5.6e^{-0.23x1} + 67.3e^{-3.05x1})
\tag{8a}
$$

$$
H_1 = \rho V^2 / 2; \; x1 = 4(L_{C1A} + L_{C1B})\eta_1 / d_1
\tag{8b}
$$

To meet the system requirement of allowable maximal pressure drop (Δp_a), the mean pressure drop (Δp_1) should be governed as

$$
(\Delta p_a) \geq \Delta p_1
\tag{9}
$$

2. A Two-Chamber Plug Muffler

As indicated in Section III.1, the total transfer matrix assembled by multiplication is

$$
\begin{pmatrix} p_1 \\ \rho_o c_o u_1 \end{pmatrix}
$$

$$
= e^{-jk\left[\frac{M_1(L_1+L_{1A})}{1-M_1^2}+\frac{M_4(L_{2A}+L_{1B})}{1-M_4^2}+\frac{M_7(L_2+L_{2B})}{1-M_7^2}\right]}
\begin{bmatrix} TS1_{1,1} & TS1_{1,2} \\ TS1_{2,1} & TS1_{2,2} \end{bmatrix}
$$

$$
\begin{bmatrix} TPE2_{1,1} & TPE2_{1,2} \\ TPE2_{2,1} & TPE2_{2,2} \end{bmatrix}
\begin{bmatrix} TPC3_{1,1} & TPC3_{1,2} \\ TPC3_{2,1} & TPC3_{2,2} \end{bmatrix}
\begin{bmatrix} TS4_{1,1} & TS4_{1,2} \\ TS4_{2,1} & TS4_{2,2} \end{bmatrix}
$$

$$
\begin{bmatrix} TPE5_{1,1} & TPE5_{1,2} \\ TPE5_{2,1} & TPE5_{2,2} \end{bmatrix}
\begin{bmatrix} TPC6_{1,1} & TPC6_{1,2} \\ TPC6_{2,1} & TPC6_{2,2} \end{bmatrix}
\begin{bmatrix} TS7_{1,1} & TS7_{1,2} \\ TS7_{2,1} & TS7_{2,2} \end{bmatrix}
$$

$$
\begin{pmatrix} p_7 \\ \rho_o c_o u_7 \end{pmatrix}
\tag{10}
$$

The sound transmission loss (*STL*) is

$$
STL_2(Q, f, Aff_{21}, Aff_{22}, Aff_{23}, Aff_{24}, Aff_{25}, Aff_{26}, Aff_{27}, Aff_{28},
$$

$$
Aff_{29}, \eta_1, dh_1)
$$

$$
= 20\log\left(\frac{\left|T_{11}^* + T_{12}^* + T_{21}^* + T_{22}^*\right|}{2}\right) + 10\log\left(\frac{S_1}{S_7}\right)
\tag{11a}
$$

where

$$
Aff_{21} = L_Z / L_o; \; Aff_{22} = L_{Z1} / L_Z; \; Aff_{23} = L_{Z1A} / L_{Z1};
$$

$$
Aff_{24} = L_{Z2A}/L_{Z2}; \; Aff_{25} = L_{C1A}/L_{Z1A}; \; Aff_{26} = L_{C1B}/L_{Z1B};
$$

$$
Aff_{27} = L_{C2A}/L_{Z2A}; \; Aff_{28} = L_{C2B}/L_{Z2B}; \; Aff_{29} = d_1/D_o;
$$

$$
L_{Z2} = L_Z - L_{Z1}; \; L_{Z1B} = L_{Z1} - L_{Z1A}; \; L_{1A} = L_{Z1A} - L_{C1A};
$$

$$
L_{1B} = L_{Z1B} - L_{C1B}; \; L_{2A} = L_{Z2A} - L_{C2A}; \; L_{2B} = L_{Z2B} - L_{C2B};
$$

$$
L_1 = L_2 = (L_o - L_Z)/2
\tag{11b}
$$

The mean pressure drop (Δp_2) of a two-chamber plug muffler is

$$
\Delta p_2 = H_{2*}[(5.6e^{-0.23x1} + 67.3e^{-3.05x1}) + (5.6e^{-0.23x2} + 67.3e^{-3.05x2})]
\tag{12a}
$$

$$
H_2 = \rho V^2 / 2;
$$

$$
x_1 = 4(L_{C1A} + L_{C1B})\eta_1 / D_1; \; x_2 = 4(L_{C2A} + L_{C2B})\eta_1 / d_1
\tag{12b}
$$

Similarly, the mean pressure drop (Δp_2) is governed as

$$
(\Delta p_a) \geq \Delta p_2
\tag{13}
$$

3. A Three-Chamber Plug Muffler

Similarly, the total transfer matrix assembled by multiplication is

$$
\begin{pmatrix} p_1 \\ \rho_o c_o u_1 \end{pmatrix}
$$

$$
= e^{-jk\left[\frac{M_1(L_1+L_{1A})}{1-M_1^2}+\frac{M_4(L_{2A}+L_{1B})}{1-M_4^2}+\frac{M_7(L_{3A}+L_{2B})}{1-M_7^2}+\frac{M_{10}(L_2+L_{3B})}{1-M_{10}^2}\right]}
\begin{bmatrix} TS1_{1,1} & TS1_{1,2} \\ TS1_{2,1} & TS1_{2,2} \end{bmatrix}
$$

$$
\begin{bmatrix} TPE2_{1,1} & TPE2_{1,2} \\ TPE2_{2,1} & TPE2_{2,2} \end{bmatrix}
\begin{bmatrix} TPC3_{1,1} & TPC3_{1,2} \\ TPC3_{2,1} & TPC3_{2,2} \end{bmatrix}
\begin{bmatrix} TS4_{1,1} & TS4_{1,2} \\ TS4_{2,1} & TS4_{2,2} \end{bmatrix}
$$

$$
\begin{bmatrix} TPE5_{1,1} & TPE5_{1,2} \\ TPE5_{2,1} & TPE5_{2,2} \end{bmatrix}
\begin{bmatrix} TPC6_{1,1} & TPC6_{1,2} \\ TPC6_{2,1} & TPC6_{2,2} \end{bmatrix}
\begin{bmatrix} TS7_{1,1} & TS7_{1,2} \\ TS7_{2,1} & TS7_{2,2} \end{bmatrix}
$$

$$
\begin{bmatrix} TPE8_{1,1} & TPE8_{1,2} \\ TPE8_{2,1} & TPE8_{2,2} \end{bmatrix}
\begin{bmatrix} TPC9_{1,1} & TPC9_{1,2} \\ TPC9_{2,1} & TPC9_{2,2} \end{bmatrix}
\begin{bmatrix} TS10_{1,1} & TS10_{1,2} \\ TS10_{2,1} & TS10_{2,2} \end{bmatrix}
$$

$$
\begin{pmatrix} p_{11} \\ \rho_o c_o u_{11} \end{pmatrix} \tag{14}
$$

Likewise, the related sound transmission loss (*STL*) is

$$
STL_3 \begin{pmatrix} Q, f, Aff_{31}, Aff_{32}, Aff_{33}, Aff_{34}, Aff_{35}, Aff_{36}, \\ Aff_{37}, Aff_{38}, Aff_{39}, Aff_{40}, Aff_{41}, Aff_{42}, \eta_1, dh_1 \end{pmatrix}
$$

$$
= 20\log\left(\frac{|T_{11}^* + T_{12}^* + T_{21}^* + T_{22}^*|}{2}\right) + 10\log\left(\frac{S_1}{S_{10}}\right) \tag{15a}
$$

where

$Aff_{31} = L_Z/L_o$; $Aff_{32} = L_{Z2}/L_Z$; $Aff_{33} = L_{Z1A}/L_{Z1}$;

$Aff_{34} = L_{Z2A}/L_{Z2}$; $Aff_{35} = L_{Z3A}/L_{Z3}$; $Aff_{36} = L_{C1A}/L_{Z1A}$;

$Aff_{37} = L_{C1B}/L_{Z1B}$; $Aff_{38} = L_{C2A}/L_{Z2A}$; $Aff_{39} = L_{C2B}/L_{Z2B}$;

$Aff_{40} = L_{C3A}/L_{Z3A}$; $Aff_{41} = L_{C3B}/L_{Z3B}$; $Aff_{42} = d_1/D_o$;

$L_{Z1} = L_{Z3} = (L_Z - L_{Z2})/2$; $L_{Z1B} = L_{Z1} - L_{Z1A}$; $L_{1A} = L_{Z1A} - L_{C1A}$;

$L_{1B} = L_{Z1B} - L_{C1B}$; $L_{2A} = L_{Z2A} - L_{C2A}$; $L_{2B} = L_{Z2B} - L_{C2B}$;

$L_{3A} = L_{Z3A} - L_{C3A}$; $L_{3B} = L_{Z3B} - L_{C3B}$; $L_1 = L_2 = (L_o - L_Z)/2$

$$\tag{15b}$$

The mean pressure drop (Δp_3) of a three-chamber plug muffler is

$$
\Delta p_3 = H_{3*}[(5.6e^{-0.23x1} + 67.3e^{-3.05x1}) + (5.6e^{-0.23x2} + 67.3e^{-3.05x2})
$$

$$
+ (5.6e^{-0.23x3} + 67.3e^{-3.05x3})]
$$

$$
H_3 = \rho V^2/2; \, x_1 = 4(L_{C1A} + L_{C1B})\eta_1/D_1;
$$

$$
x_2 = 4(L_{C2A} + L_{C2B})\eta_1/d_1; x_3 = 4(L_{C3A} + L_{C3B})\eta_1/d_1 \tag{16}
$$

Also, the mean pressure drop (Δp_3) is governed as

$$
(\Delta p_a) \geq \Delta p_3 \tag{17}
$$

4. Overall Sound Power Level

The silenced octave sound power level emitted from a silencer's outlet is

$$
SWL_i = SWLO_i - STL_i \tag{18}
$$

where

(1) The $SWLO_i$ is the original *SWL* at the inlet of a muffler (or pipe outlet), and i is the index of the octave band frequency.
(2) The STL_i is the muffler's *STL* with respect to the relative octave band frequency.
(3) The SWL_i is the silenced *SWL* at the outlet of a muffler with respect to the relative octave band frequency.

Finally, the overall SWL_T silenced by a muffler at the outlet is

$$
SWL_T = 10*\log\{\sum_{i=1}^{8} 10^{SWL_i/10}\}
$$

$$
= 10*\log\left\{
\begin{array}{l}
10^{[SWLO(f=63)-STL(f=63)]/10} + 10^{[SWLO(f=125)-STL(f=125)]/10} + 10^{[SWLO(f=250)-STL(f=250)]/10} \\
+10^{[SWLO(f=500)-STL(f=500)]/10} + 10^{SWLO(f=1000)-STL(f=1000)]/10} + 10^{SWLO(f=2000)-STL(f=2000)]/10} \\
+10^{[SWLO(f=4000)-STL(f=4000)]/10}
\end{array}
\right\}
$$

$$\tag{19}$$

5. Objective Function

By using the formulas of (7), (9), (11), (13), (15), (17), and (19), the objective function used in the GA optimization with respect to each type of plug muffler was established.

For a single-chamber plug muffler, the objective function in maximizing the STL at a pure tone (f) is

$$
OBJ_{11} = STL_1(Q, f, Aff_{11}, Aff_{12}, Aff_{13}, Aff_{14}, Aff_{15}, \eta_1, dh_1, \Delta p_1)
$$

$$
= 20\log\left(\frac{|T_{11}^* + T_{12}^* + T_{21}^* + T_{22}^*|}{2}\right) + 10\log\left(\frac{S_1}{S_4}\right) \tag{20a}
$$

To minimize the overall SWL, the objective function is

$$OBJ_{12} = SWL_T(Q, Aff_{11}, Aff_{12}, Aff_{13}, Aff_{14}, Aff_{15}, \eta_1, dh_1, \Delta p_1)$$

$$= 20\log\left(\frac{\left|T_{11}^* + T_{12}^* + T_{21}^* + T_{22}^*\right|}{2}\right) + 10\log\left(\frac{S_1}{S_4}\right) \quad (20b)$$

Similarly, for a double-chamber plug muffler, the objective function in maximizing the STL at a pure tone (f) is

$$OBJ_{21} = STL_2\left(\begin{array}{c} Q, f, Aff_{21}, Aff_{22}, Aff_{23}, Aff_{24}, Aff_{25}, Aff_{26}, \\ Aff_{27}, Aff_{28}, Aff_{29}, \eta_1, dh_1, \Delta p_2 \end{array}\right)$$

$$= 20\log\left(\frac{\left|T_{11}^* + T_{12}^* + T_{21}^* + T_{22}^*\right|}{2}\right) + 10\log\left(\frac{S_1}{S_7}\right) \quad (21a)$$

Likewise, the minimized objective function with respect to the SWL in a double-chamber plug muffler is

$$OBJ_{22} = SWL_T\left(\begin{array}{c} Q, Aff_{21}, Aff_{22}, Aff_{23}, Aff_{24}, Aff_{25}, Aff_{26}, \\ Aff_{27}, Aff_{28}, Aff_{29}, \eta_1, dh_1, \Delta p_2 \end{array}\right)$$

$$= 20\log\left(\frac{\left|T_{11}^* + T_{12}^* + T_{21}^* + T_{22}^*\right|}{2}\right) + 10\log\left(\frac{S_1}{S_7}\right) \quad (21b)$$

Equally, for the three-chamber plug muffler, the objective function in maximizing the STL at a pure tone (f) is

$$OBJ_{31} = STL_3\left(\begin{array}{c} Q, f, Aff_{31}, Aff_{32}, Aff_{33}, Aff_{34}, Aff_{35}, Aff_{36}, \\ Aff_{37}, Aff_{38}, Aff_{39}, Aff_{40}, Aff_{41}, Aff_{42}, \eta_1, dh_1, \Delta p_3 \end{array}\right)$$

$$= 20\log\left(\frac{\left|T_{11}^* + T_{12}^* + T_{21}^* + T_{22}^*\right|}{2}\right) + 10\log\left(\frac{S_1}{S_{10}}\right) \quad (22a)$$

The related objective function in minimizing the overall SWL is

$$OBJ_{32} = STL_3\left(\begin{array}{c} Q, Aff_{31}, Aff_{32}, Aff_{33}, Aff_{34}, Aff_{35}, Aff_{36}, Aff_{37}, \\ Aff_{38}, Aff_{39}, Aff_{40}, Aff_{41}, Aff_{42}, \eta_1, dh_1, \Delta p_3 \end{array}\right)$$

$$= 20\log\left(\frac{\left|T_{11}^* + T_{12}^* + T_{21}^* + T_{22}^*\right|}{2}\right) + 10\log\left(\frac{S_1}{S_{10}}\right) \quad (22b)$$

III. MODEL CHECKS

Before performing the *GA* optimal simulation on mufflers,
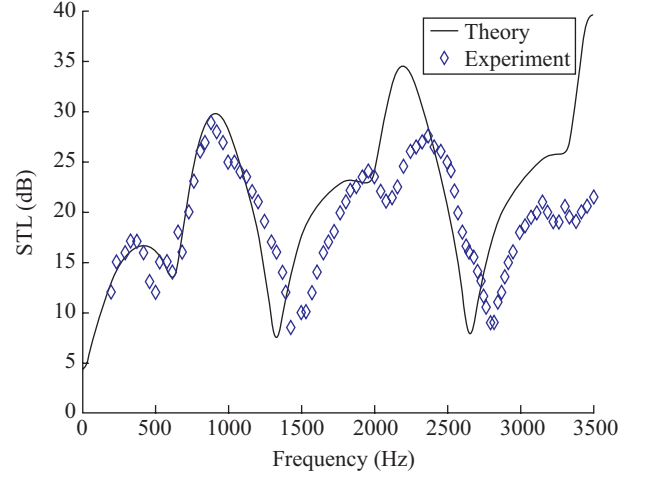
Fig. 4. Performance of a one-chamber perforated plug muffler with the mean flow [$M_1 = M_2 = 0.05$, $D_1 = 0.0493$ (m), $Do = 0.1016$ (m), $L_{C1} = L_{C2} = 0.1286$ (m), $L_1 = L_2 = 0.1$ (m), $L_{A1} = L_{B2} = 0.0$ (m), $t = 0.081$ (m), $dh_1 = dh_2 = 0.00249$ (m), $\eta_1 = \eta_2 = 0.037$] [Experiment data is from Sullivan[13, 15, 19]].

accuracy checks of the mathematical models on a single-chamber plug perforated muffler are performed using the experimental data from Sullivan [13, 15, 16]. As depicted in Fig. 4, the performance curves with respective to theoretical and experiment data are relatively accurate and in agreement. Based on plane wave theory, the proposed theoretical cutoff frequency of fc_1 $\left(f_{c1} = \dfrac{1.84 c_o}{\pi D}(1 - M^2)^{1/2}\right)$ is 1974 Hz.

Therefore, the proposed fundamental mathematical models with related acoustical components are acceptable. Consequently, the models linked with the numerical method are applied to the shape optimization in the following section.

IV. CASE STUDIES

In this paper, a blower confined within a RC (reinforced concrete) room is shown in Fig. 1. The noise level in the equipment venting outlet is remarkable. To efficiently depress the noise, the multi-chamber plug muffler hybridized with perforated tubes is considered. The spectrum of the exhaust sound power level (*SWL*) at the muffler inlet is

f (Hz)	125	250	500	1k	2k	4k	Overall SWL
SWL (dB)	128	135	126	115	108	100	136.3

**Table 1. Range of design parameters for three kinds of multi-chamber plug mufflers.**

Muffler Type	Range of design parameters
One-Chamber	Targeted f: {250, 550, 750}; Q = 0.01 (m³/s); D_o = 0.5 (m); Lo = 1.8 (m); Aff_{11}: [0.5, 0.9]; Aff_{12}: [0.3, 0.7]; Aff_{13}: [0.5, 0.9]; Aff_{14}: [0.5, 0.9]; Aff_{15}: [0.5, 0.6]; η_1: [0.03, 0.1]; dh_1: [0.00175, 0.007]; Δp_a: 800 (Pa)
Two-Chamber	Targeted f: {250, 550, 750}; Q = 0.01 (m³/s); D_o = 0.5 (m); Lo = 1.8 (m); Aff_{21}: [0.5, 0.9]; Aff_{22}: [0.3, 0.7]; Aff_{23}: [0.3, 0.7]; Aff_{24}: [0.3, 0.7]; Aff_{25}: [0.5, 0.9]; Aff_{26}: [0.5, 0.9]; Aff_{27}: [0.5, 0.9]; Aff_{28}: [0.5, 0.9]; Aff_{29}: [0.5, 0.6]; η_1: [0.03, 0.1]; dh_1: [0.00175, 0.007]; Δp_a: 800 (Pa)
Three-Chamber	Targeted f: {250, 550, 750}; Q = 0.01 (m³/s); D_o = 0.5 (m); Lo = 1.8 (m); Aff_{31}: [0.5, 0.9]; Aff_{32}: [0.3, 0.7]; Aff_{33}: [0.3, 0.7]; Aff_{34}: [0.3, 0.7]; Aff_{35}: [0.3, 0.7]; Aff_{36}: [0.5, 0.9]; Aff_{37}: [0.5, 0.9]; Aff_{38}: [0.5, 0.9]; Aff_{39}: [0.5, 0.6]; Aff_{40}: [0.5, 0.9]; Aff_{41}: [0.5, 0.9]; Aff_{42}: [0.3, 0.7]; η_1: [0.03, 0.1]; dh_1: [0.00175, 0.007]; Δp_a: 800 (Pa)

Before the minimization of a broadband noise is performed, the maximization of the STL with respect to three kinds of perforated plug mufflers at various targeted pure tones (250, 550, 750 Hz) has been performed for the purpose of an accuracy check on the GA method. As shown in Fig. 1, the available space for a muffler is 0.5 m in width, 0.5 m in height, and 1.8 m in length. In the existing venting system, the flow rate (Q) and thickness of the perforated tube (t) are given as 0.01 (m³/s) and 0.0015 (m). To prevent overloading back pressure which will slow down the preset volume- flow-rate (Q), the allowable maximal Δp of 800 (Pa) in the muffler system is specified in advance. The corresponding space constraints and the ranges of the design parameters for each muffler are summarized in Table 1.

V. GENETIC ALGORITHM

The concept of Genetic Algorithms, first formalized by Holland [6] and then extended to functional optimization by Jong [8], involves the use of optimization search strategies patterned after the Darwinian notion of natural selection.

For the optimization of the objective function (*OBJ*), the design parameters of $(X_1, X_2,…, X_k)$ were determined. When the *bit* (the bit length of the chromosome) was chosen, the interval of the design parameter (X_k) with $[Lb, Ub]_k$ was then mapped to the band of the binary value. The mapping system between the variable interval of $[Lb, Ub]_k$ and the kth binary chromosome of

$$\underbrace{0\ 0\ 0\ 0\ \bullet\ \bullet\ \bullet\ 0\ 0\ 0}_{bit} \sim \underbrace{1\ 1\ 1\ 1\ \bullet\ \bullet\ \bullet\ 1\ 1\ 1}_{bit}$$
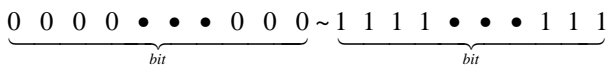
was then built. The encoding from x to *B2D* (binary to decimal) can be performed as

$$B2D_k = \text{integer}\left\{ \frac{x_k - Lb_k}{Ub_k - Lb_k}(2^{bit} - 1) \right\} \tag{23}$$

The initial population was built up by randomization. The parameter set was encoded to form a string which represented the chromosome. By evaluating the objective function (*OBJ*),
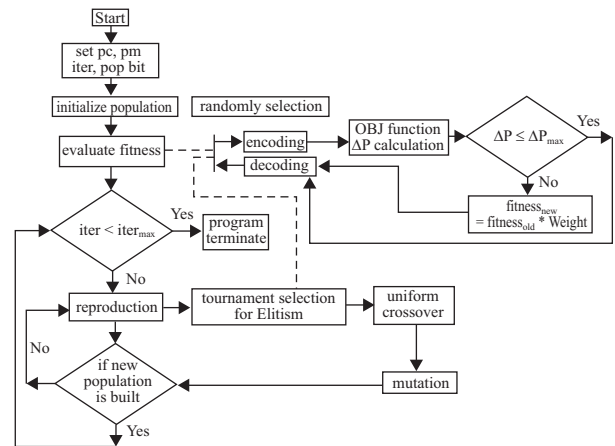
Fig. 5. The block diagram of the GA optimization on mufflers.

the whole set of chromosomes $[B2D_1, B2D_2, …., B2D_k]$ that changed from binary form to decimal form was then assigned a fitness by decoding the transformation system.

$$fitness = OBJ(X_1, X_2, …, X_k) \tag{24a}$$

where

$$X_k = B2D_k * (Ub_k - Lb_k)/(2^{bit} - 1) + Lb_k \tag{24b}$$

As the block diagram indicates in Fig. 5, during the decoding process, the back pressure (Δp) will be calculated and compared with the limit of Δp_a. If Δp is smaller than Δp_a, the current offspring will be valid and used for further evolution. If this is not the case, fitness will be weighted to discard the current gene.

As indicated in Fig. 6, to process the elitism of a gene, the tournament selection, a random comparison of the relative fitness from pairs of chromosomes, was applied. During the GA optimization, one pair of offspring from the selected parent was generated by uniform crossover with a probability of *pc*. Genetically, mutation occurred with a probability of *pm* where the new and unexpected point was brought into the GA optimizer's search domain. To prevent the best gene from
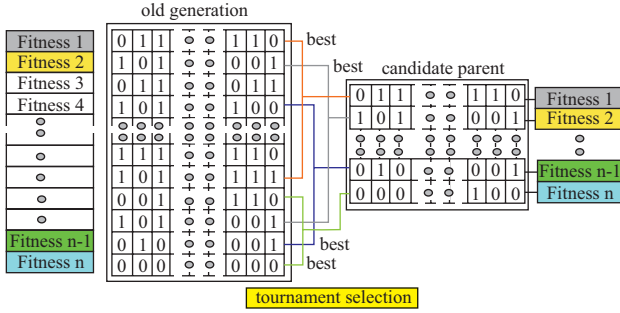
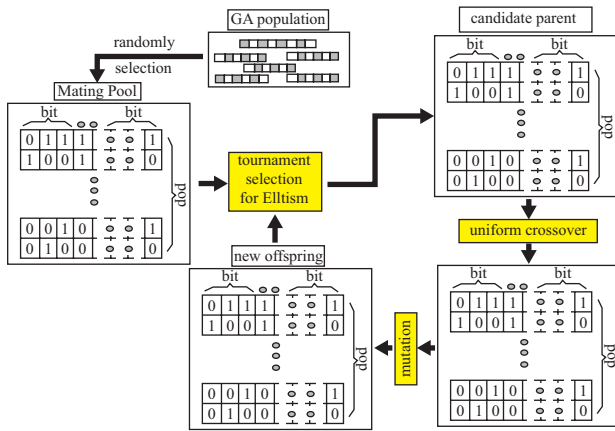**Fig. 6. Scheme of elitism by tournament selection.**

Fig. 7. Operations in the GA method.

disappearing and to improve the accuracy of optimization during reproduction, the elitism scheme of keeping the best gene (one pair) in the parent generation with the tournament strategy was developed.

The process was terminated when a number of generations exceeded a pre-selected value of *genno*. The operations in the GA method are pictured in Fig. 7.

To simplify the optimization for three kinds of plug mufflers, the flow rate (Q = 0.01 (m³/s)) and thickness of the perforated tube ($t_1 = t_2 = 0.0081$ (m)) are preset in advance; therefore, Eqs. (20), (21), (22), the objective functions (OBJ_{11}, OBJ_{12}, OBJ_{21}, OBJ_{22}, OBJ_{31} and OBJ_{32}) and their ranges are reduced and set as

$$OBJ_{11}(X_1, X_2, X_3, X_4, X_5, X_6, X_7, X_8)$$
$$= STL(aff_{11}, aff_{12}, aff_{13}, aff_{14}, aff_{15}, \eta_1, dh_1, \Delta p_a) \tag{25a}$$

$$OBJ_{12}(X_1, X_2, X_3, X_4, X_5, X_6, X_7, X_8)$$
$$= SWL_T(aff_{11}, aff_{12}, aff_{13}, aff_{14}, aff_{15}, \eta_1, dh_1, \Delta p_a) \tag{25b}$$

$$OBJ_{21}(X_1, X_2, X_3, X_4, X_5, X_6, X_7, X_8, X_9, X_{10}, X_{11}, X_{12})$$
$$= STL(aff_{21}, aff_{22}, aff_{23}, aff_{24}, aff_{25}, aff_{26}, aff_{27}, aff_{28},$$
$$aff_{29}, \eta_1, dh_1, \Delta p_a) \tag{26a}$$

$$OBJ_{22}(X_1, X_2, X_3, X_4, X_5, X_6, X_7, X_8, X_9, X_{10}, X_{11}, X_{12})$$
$$= SWL_T(aff_{21}, aff_{22}, aff_{23}, aff_{24}, aff_{25}, aff_{26}, aff_{27}, aff_{28},$$
$$aff_{29}, \eta_1, dh_1, \Delta p_a) \tag{26b}$$

$$OBJ_{31}(X_1, X_2, X_3, X_4, X_5, X_6, X_7, X_8, X_9, X_{10}, X_{11}, X_{12},$$
$$X_{13}, X_{14}, X_{15})$$
$$= STL(aff_{31}, aff_{32}, aff_{33}, aff_{34}, aff_{35}, aff_{36}, aff_{37}, aff_{38}, aff_{39},$$
$$aff_{40}, aff_{41}, aff_{42}, \eta_1, dh_1, \Delta p_a) \tag{27a}$$

$$OBJ_{32}(X_1, X_2, X_3, X_4, X_5, X_6, X_7, X_8, X_9, X_{10}, X_{11}, X_{12},$$
$$X_{13}, X_{14}, X_{15})$$
$$= SWL_T(aff_{31}, aff_{32}, aff_{33}, aff_{34}, aff_{35}, aff_{36}, aff_{37}, aff_{38}, aff_{39},$$
$$aff_{40}, aff_{41}, aff_{42}, \eta_1, dh_1, \Delta p_a) \tag{27b}$$

VI. RESULTS AND DISCUSSION

1. Results

To achieve good optimization, five kinds of optimal GA parameters, including population size (*pop*), chromosome length (*bit*), maximum generation (*iter*ₘₐₓ), crossover ratio (*pc*), and mutation ratio (*pm*) are obtained by varying their values during optimization. The optimization system is encoded by Fortran and run on an IBM PC - Pentium IV. The results of two kinds of optimizations — one of the pure tone noise used for GA's accuracy check and the other of broadband noise occurring in a blower room — are described below.

1) Pure Tone Noise Optimization
A. One-Chamber Plug Muffler

For a one-chamber plug muffler, various sets of *GA* parameters are tested during optimal process. The resultant simulated result optimized with respect to the pure tone of 250Hz is shown in Table 2. As indicated in Table 2, the optimal design data can be obtained when the *GA* parameters at *pop*, *bit*, *iter*ₘₐₓ, *pc*, and *pm* = 80, 10, 200, 0.6, 0.05 are applied. Using this GA parameter set with two other pure tones (550, 750 Hz), the muffler's optimal sizes with respect to various pure tones are summarized in Table 3. Using the optimal design in a theoretical calculation, three optimal STL curves with respect to targeted frequencies are plotted and depicted in Fig. 8. As revealed in Fig. 8, the STLs are precisely maximized at the desired frequencies. The related mufflers' sizes with respect to three kinds of pure tones (250, 550, 750 Hz) are shown in Figs. 9-11.

To appreciate the influence of the STL and Δp with respect to other parameters, a simple sensitivity analysis using seven
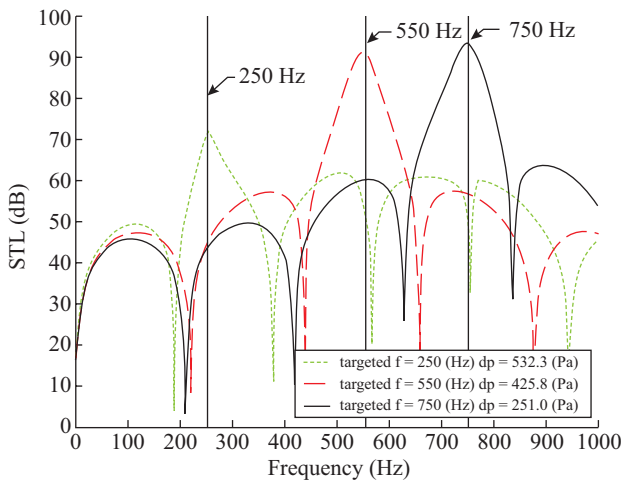
Table 2. Optimal STLs for a one-chamber plug perforated muffler (targeted frequency: 250 Hz).

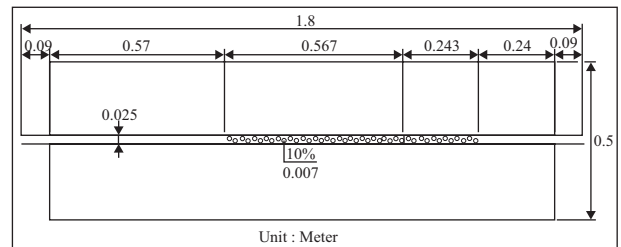| Optimal GA parameters					Optimal Result				
pop	*bit*	*pm*	*pc*	$iter_{max}$	Aff_{11}	Aff_{12}	Aff_{13}	Aff_{14}	STL (dB)
					0.9000	0.7000	0.5000	0.5000	71.299
80	10	0.05	0.6	200	Aff_{15}	η_1	dh_1 (m)		Δp (Pa)
					0.0500	0.1000	0.0070		532.3
Notes: Aff_{11} = Lz/Lo; Aff_{12} = Lz1A/Lz; Aff_{13} = Lc1A; Aff_{14} = Lc1B/Lz1B; Aff_{15} = d1/Do									

Table 3. Optimal STLs for a one-chamber plug perforated muffler with respect to various targeted frequencies (with Δp constraint).

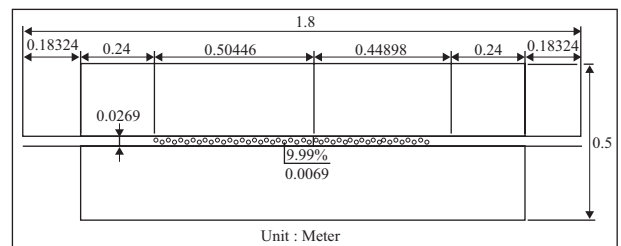| Item	Targeted frequency	Results				
		Aff_{11}	Aff_{12}	Aff_{13}	Aff_{14}	STL (dB)
1	250 Hz	0.9000	0.7000	0.5000	0.5000	**71.299**
		Aff_{15}	η_1	dh_1 (m)		Δp (Pa)
		0.0500	0.1000	0.0070		**532.3**
2	550 Hz	Aff_{11}	Aff_{12}	$Aff13$	Aff_{14}	STL (dB)
		0.7964	0.5194	0.6775	0.6517	**91.857**
		Aff_{15}	η_1	dh_1 (m)		Δp (Pa)
		0.0538	0.0999	0.0069		**340.5**
3	750 Hz	Aff_{11}	Aff_{12}	Aff_{13}	Aff_{14}	STL (dB)
		0.8128	0.5174	0.7796	0.7639	**93.536**
		Aff_{15}	η_1	dh_1 (m)		Δp (Pa)
		0.0532	0.0995	0.0066		**251.0**

Fig. 8. Optimal STL with respect to frequencies for a one-chamber plug silencer [targeted frequency: 250, 550 and 750 Hz].

Fig. 9. Optimal shape of a one-chamber plug muffler with a targeted frequency of 250 Hz.

Fig. 10. Optimal shape of a one-chamber plug muffler with a targeted frequency of 550 Hz.

parameters (Aff_{11}, Aff_{12}, Aff_{13}, Aff_{14}, Aff_{15}, η_1, and dh_1) for a one-chamber plug muffler at a targeted frequency of 250 (Hz) is performed and shown in Figs. 12-18. As indicated in Figs. 12-18, it is obvious that the STL is inversely proportional to the diameter of the inner duct (Aff_{15}) and to the lengths of the perforated ducts (Aff_{13}, Aff_{14}). Moreover, the back pressure Δp will obviously decrease when either the length of the chamber (Aff_{11}), the lengths of the perforated ducts (Aff_{13}, Aff_{14}), the

diameter of the inner duct (Aff_{15}), or the porosity of the inner duct (η_1) is increased. Because the decrement of the parameters (Aff_{13}, Aff_{14} Aff_{15}) will result in the increment of both the

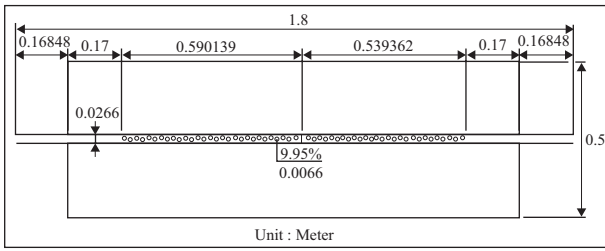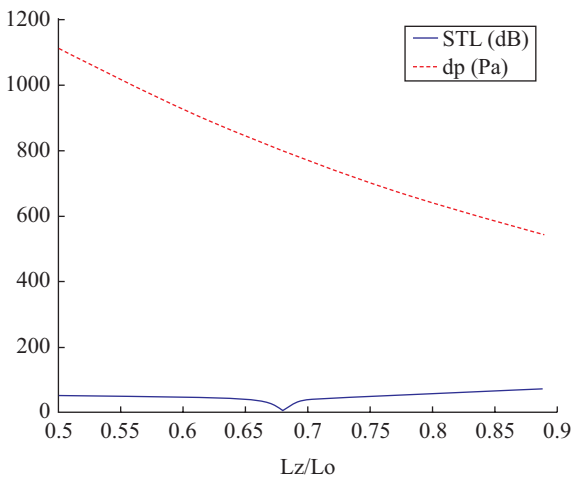**Fig. 11. Optimal shape of a one-chamber plug muffler with a targeted frequency of 750 Hz.**

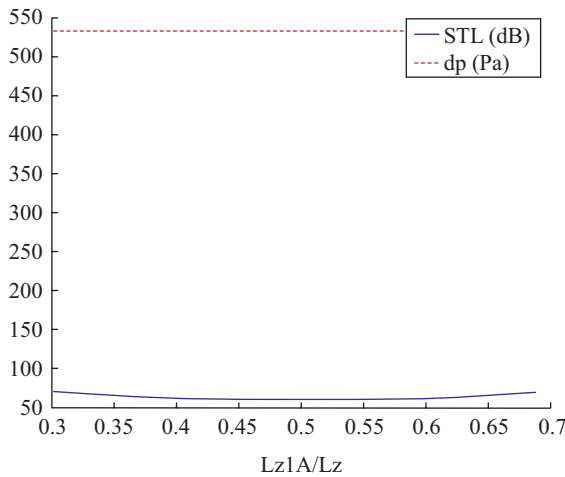**Fig. 12. Influence of Aff_{11}(Lz/Lo) on a STL and a Δp with a targeted frequency of 250 Hz.**

Fig. 13. Influence of Aff_{12}(Lz1A/Lz) on a STL and a Δp with a targeted frequency of 250 Hz.

Fig. 14. Influence of Aff_{13}(Lc1A/Lz1A) on a STL and a Δp with a targeted frequency of 250 Hz.

Fig. 15. Influence of Aff_{14}(Lc1B/Lz1B) on a STL and a Δp with a targeted frequency of 250 Hz.
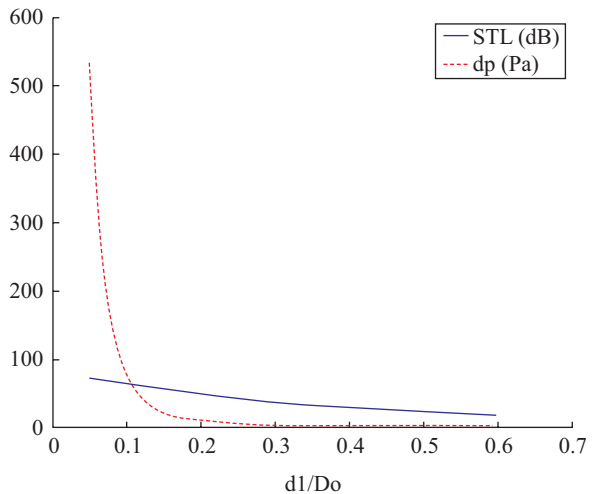
Fig. 16. Influence of Aff_{15}(d1/Do) on a STL and a Δp with a targeted frequency of 250 Hz.

STL and Δp simultaneously, a compromise between these parameters during the numerical optimization process will be required. Therefore, to reach a higher STL with a Δp below the allowable maximal pressure drop, an appropriate decrement of the Aff_{13}, Aff_{14} Aff_{15} is essential. As indicated in Table
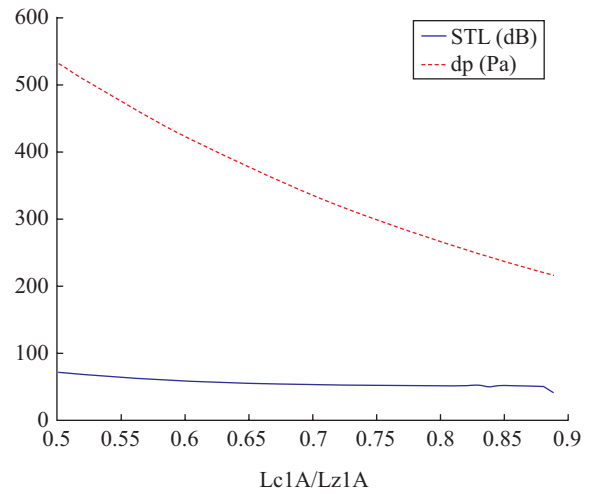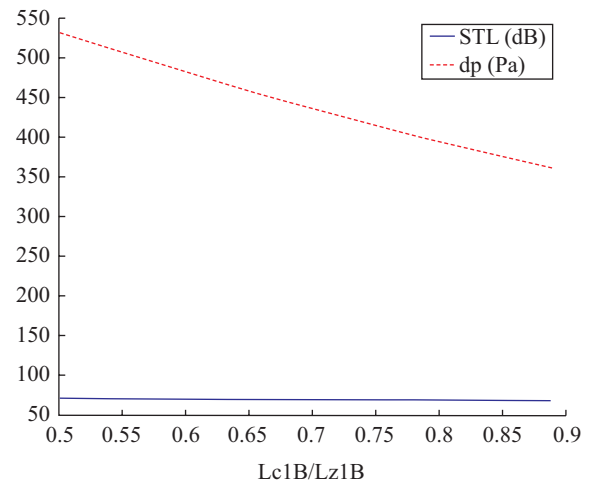
Table 4. Optimal STLs for a two-chamber plug perforated muffler (targeted frequency: 250 Hz).

Optimal GA parameters					Optimal Result				
pop	*bit*	*pm*	*pc*	*iter*$_{max}$	Aff_{21}	Aff_{22}	Aff_{23}	Aff_{24}	STL (dB)
					0.5000	0.3000	0.7000	0.7000	104.1
					Aff_{25}	Aff_{26}	Aff_{27}	Aff_{28}	Δp (Pa)
80	25	0.05	0.6	500	0.5000	0.5000	0.5125	0.5000	800.0
					Aff_{29}	η$_1$	dh_1 (m)		
					0.1330	0.0300	0.0018		

Notes: Aff_{21} = Lz/Lo; Aff_{22} = Lz1/Lz; Aff_{23} = Lz1A/Lz1; Aff_{24} = Lz2A/Lz2; Aff_{25} = Lc1A/Lz1A; Aff_{26} = Lc1B/Lz1B; Aff_{27} = Lc2A/Lz2A; Aff_{28} = Lc2B/Lz2B; Aff_{29} = d1/Do
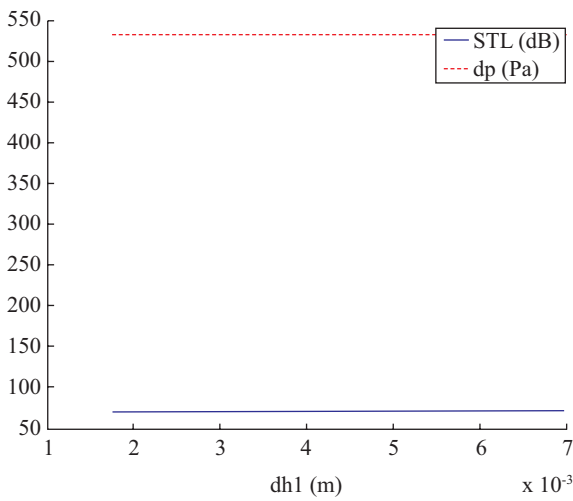
Fig. 17. Influence of dh1 on a STL and a Δp with a targeted frequency of 250 Hz.

Fig. 19. Optimal STL with respect to frequencies for a two-chamber plug silencer [targeted frequency: 250, 550 and 750 Hz].

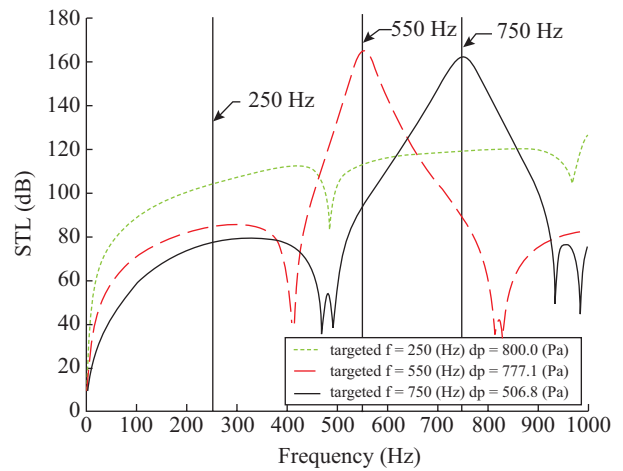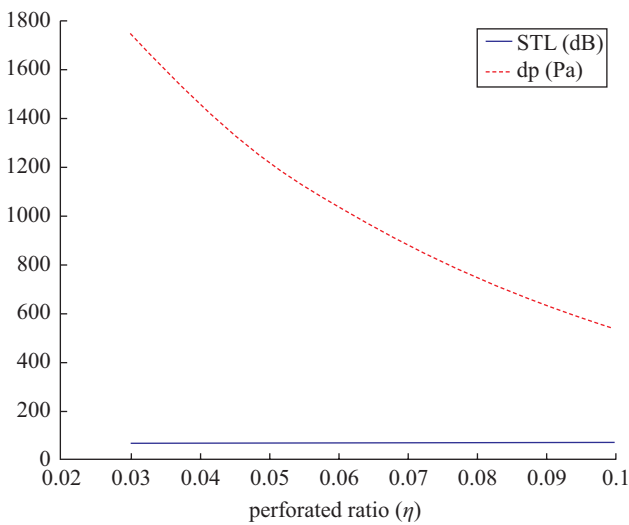**Fig. 18. Influence of η on a STL and a Δp with a targeted frequency of 250 Hz.**

For a two-chamber plug muffler, thirteen sets of *GA* parameters are tested by varying the values of the GA parameters. The optimized result with respect to the pure tone of 250 Hz is listed in Table 4. As indicated in Table 4, the optimal design data can be obtained when the *GA* parameters at *pop*, *bit*, *iter*$_{max}$, *pc*, and *pm* = 80, 25, 500, 0.6, 0.05 are used. Using this GA parameter set with two other pure tones (550, 750 Hz), the muffler's optimal sizes with respect to various pure tones are summarized in Table 5. Using the optimal design in a theoretical calculation, three optimal STL curves with respect to the targeted frequencies are plotted in Fig. 19. As revealed in Fig. 19, the STLs are precisely maximized at the desired frequencies. Moreover, it is obvious that the STL at the higher targeted frequency will be larger than the lower one. The related mufflers' sizes with respect to three kinds of pure tones (250, 550, 750 Hz) are shown in Figs. 20-22.

C. Three-Chamber Plug Muffler

For a three-chamber plug muffler, the optimized result with respect to the pure tone of 250Hz is shown in Table 6. As indicated in Table 6, the optimal design data can be obtained at the *GA* parameters (*pop*, *bit*, *iter*$_{max}$, *pc*, and *pm*) = (60, 15, 1000, 0.6 , 0.05). Using this GA parameter set with two other pure tones (550, 750 Hz), the muffler's optimal sizes with respect to various pure tones are summarized in Table 7.

3, the STL at a higher targeted frequency will be larger than that at a lower targeted frequency.

B. Two-Chamber Plug Muffler

Table 5. Optimal STLs for a two-chamber plug perforated muffler with respect to various targeted frequencies (with Δp constraint).

| Item	Targeted frequency	Optimal Results				
1	250 Hz	Aff_{21}	Aff_{22}	Aff_{23}	Aff_{24}	STL (dB)
		0.7588	0.3938	0.6984	0.3610	**87.5**
		Aff_{25}	Aff_{26}	Aff_{27}	Aff_{28}	Δp (Pa)
		0.8554	0.5540	0.5012	0.5633	**797**
		Aff_{29}	η_1	dh_1 (m)		
		0.0914	0.0430	0.0050		
2	550 Hz	Aff_{21}	Aff_{22}	Aff_{23}	Aff_{24}	STL (dB)
		0.8250	0.5046	0.4914	0.5000	**165**
		Aff_{25}	Aff_{26}	Aff_{27}	Aff_{28}	Δp (Pa)
		0.5125	0.5241	0.5000	0.5003	**777**
		Aff_{29}	η_1	dh_1 (m)		
		0.1166	0.0300	0.0070		
3	750 Hz	Aff_{21}	Aff_{22}	Aff_{23}	Aff_{24}	STL (dB)
		0.7083	0.5125	0.4750	0.5002	**162**
		Aff_{25}	Aff_{26}	Aff_{27}	Aff_{28}	Δp (Pa)
		0.5000	0.5500	0.5000	0.5000	**507**
		Aff_{29}	η_1	dh_1 (m)		
		0.0844	0.1000	0.0070		

Table 6. Optimal STLs for a three-chamber plug perforated muffler (targeted frequency: 250 Hz).

GA parameters					Optimal Results				
pop	*bit*	*pm*	*pc*	$iter_{max}$	Aff_{31}	Aff_{32}	Aff_{33}	Aff_{34}	STL (dB)
					0.500	0.7000	0.7000	0.7000	179.9
					Aff_{35}	Aff_{36}	Aff_{37}	Aff_{38}	Δp (Pa)
					0.700	0.5000	0.5000	0.5134	799.3
60	15	0.05	0.6	1000	Aff_{39}	Aff_{40}	Aff_{41}	Aff_{42}	
					0.501	0.5000	0.5000	0.1577	
					η_1	dh_1 (m)			
					0.030	0.0018			
Notes: Aff_{31} = Lz/Lo; Aff_{32} = Lz2/Lz; Aff_{33} = Lz1A/Lz1; Aff_{34} = Lz2A/Lz2; Aff_{35} = Lz3A/Lz3; Aff_{36} = Lc1A/Lz1A; Aff_{37} = Lc1B/Lz1B; Aff_{38} = Lc2A/Lz2A; Aff_{39} = Lc2B/Lz2B; Aff_{40} = Lc3A/Lz3A; Aff_{41} = Lc3B/Lz3B; Aff_{42} = d1/Do									
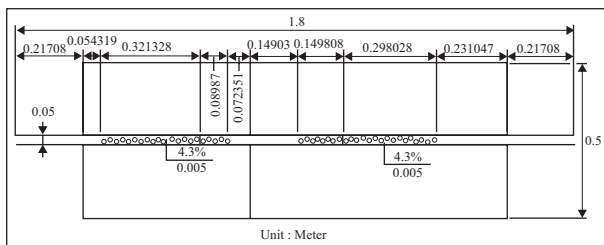
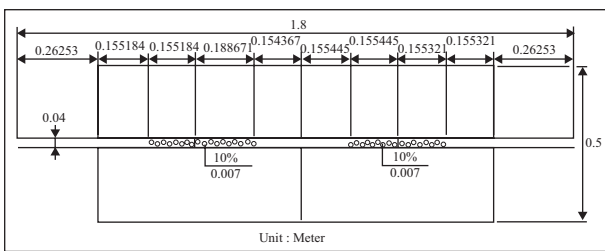**Fig. 20. Optimal shape of a two-chamber plug muffler with a targeted frequency of 250 Hz.**
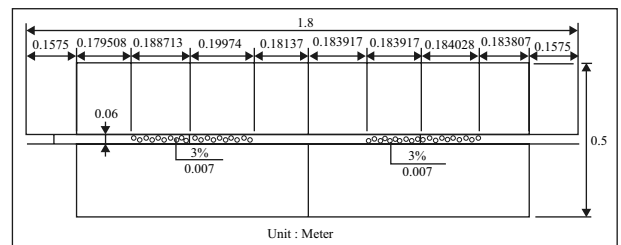
Fig. 21. Optimal shape of a two-chamber plug muffler with a targeted frequency of 550 Hz.

Using the optimal design in a theoretical calculation, three optimal STL curves with respect to the targeted frequencies are plotted in Fig. 23. As revealed in Fig. 23, the STLs are precisely maximized at the desired frequencies. The related mufflers' sizes with respect to three kinds of pure tones (250, 550, 750 Hz) are shown in Figs. 24-26. It is obvious that the

Table 7. Optimal STLs for a three-chamber plug perforated muffler with respect to various targeted frequencies (with Δp constraint).

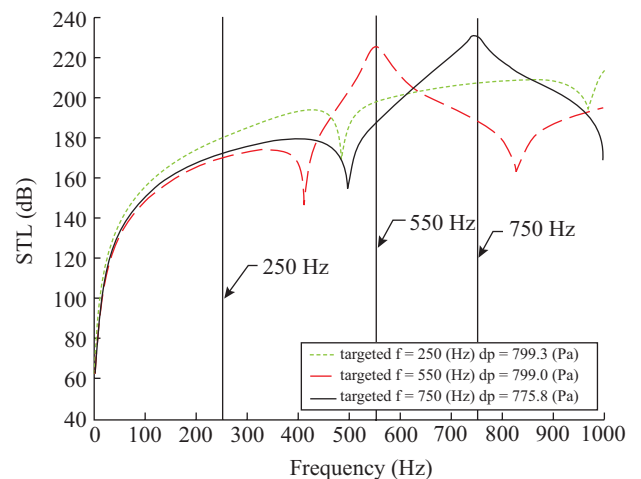| Item	Targeted frequency	Optimal Results				
		Aff_{31}	Aff_{32}	Aff_{33}	Aff_{34}	STL (dB)
		0.5559	0.6996	0.6996	0.4806	**168.8**
		Aff_{35}	Aff_{36}	Aff_{37}	Aff_{38}	Δp (Pa)
1	250 Hz	0.3004	0.5008	0.5641	.7804	**798.5**
		Aff_{39}	Aff_{40}	Aff_{41}	Aff_{42}	
		0.8984	0.5192	0.5004	0.1527	
		η_1	dh_1 (m)			
		0.0301	0.0046			
		Aff_{31}	Aff_{32}	Aff_{33}	Aff_{34}	STL (dB)
		0.5876	0.7000	0.6999	0.4997	**225.7**
		Aff_{35}	Aff_{36}	Aff_{37}	Aff_{38}	Δp (Pa)
2	550 Hz	0.6999	0.5003	0.5000	0.5001	**799.0**
		Aff_{39}	Aff_{40}	Aff_{41}	Aff_{42}	
		0.5001	0.5004	0.5001	0.1558	
		η_1	dh_1 (m)			
		0.0300	0.0070			
		Aff_{31}	Aff_{32}	Aff_{33}	Aff_{34}	STL (dB)
		0.5000	0.6807	0.3000	0.5622	**231.1**
		Aff_{35}	Aff_{36}	Aff_{37}	Aff_{38}	Δp (Pa)
3	750 Hz	0.3000	0.5001	0.5001	0.7250	**775.8**
		Aff_{39}	Aff_{40}	Aff_{41}	Aff_{42}	
		0.5000	0.5005	0.5000	0.1574	
		η_1	dh_1 (m)			
		0.0300	0.0070			

Fig. 22. Optimal shape of a two-chamber plug muffler with a targeted frequency of 750 Hz

STL at the higher targeted frequency will be larger than that at the lower one.

2) Broadband Noise Optimization

By using the above *GA* parameters, the optimal muffler's design data for three kinds of multi-chamber plug mufflers (a one-chamber, two-chamber, and a three-chamber) used to minimize the sound power level at the muffler's outlet is summarized in Table 8. As illustrated in Table 8, the resultant sound power levels with respect to three kinds of mufflers have been dramatically reduced from 136.3 dB(A) to 96.2

Fig. 23 Optimal STL with respect to frequencies for a three-chamber plug silencer [targeted frequency: 250, 550 and 750 Hz].

dB(A), 53.0 dB(A), and 11.9 dB(A). Using this optimal design in a theoretical calculation, the resultant curves of the *SWL* with respect to three kinds of mufflers are plotted in Fig. 27. As shown in Fig. 27, the muffler with three chambers
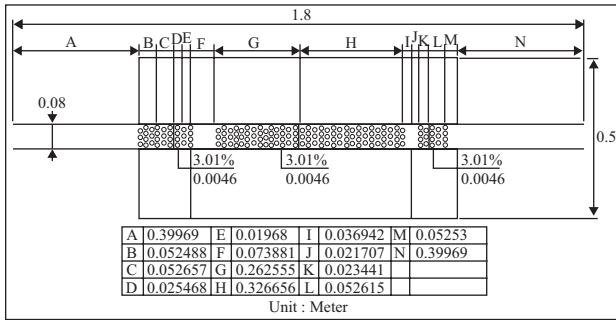
Fig. 24. Optimal shape of a three-chamber plug muffler with a targeted frequency of 250 Hz.
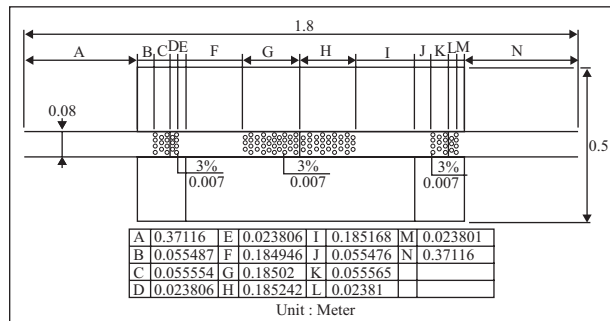

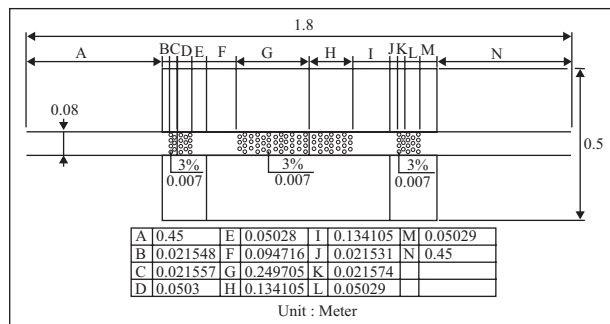**Fig. 25. Optimal shape of a three-chamber plug muffler with a targeted frequency of 550 Hz.**

Fig. 26. Optimal shape of a three-chamber plug muffler with a targeted frequency of 750 Hz.
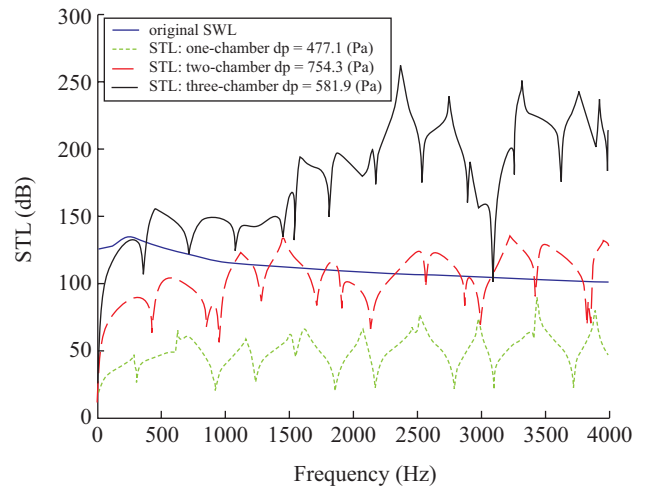

Fig. 27. A comparison of three kinds of optimal STLs with an original sound power level [broadband frequency].
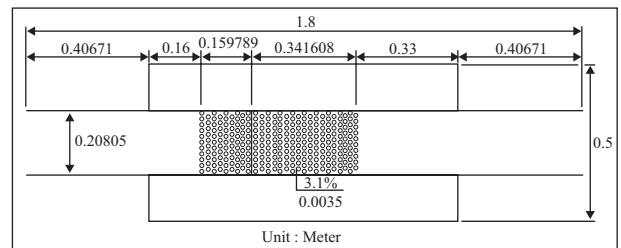

Fig. 28. Optimal shape of a one-chamber plug muffler [broadband frequency].
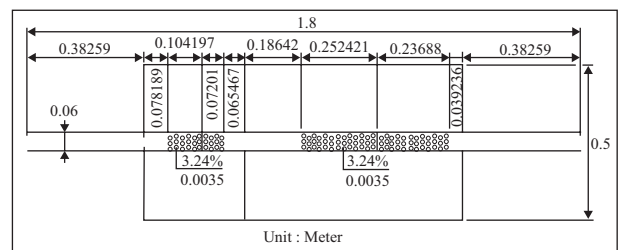

Fig. 29. Optimal shape of a two-chamber plug muffler [broadband frequency].

obviously has the best acoustical performance. Based on plane wave theory, the proposed available theoretical cutoff frequencies of fc_1 $\left(f_{c1} = \dfrac{1.84c_o}{\pi D}(1-M^2)^{1/2} \right)$ with respect to three kinds of mufflers are 964 Hz, 3220 Hz, and 1974 Hz. Consequently, the optimal mufflers' size is also shown in Figs. 28~30.
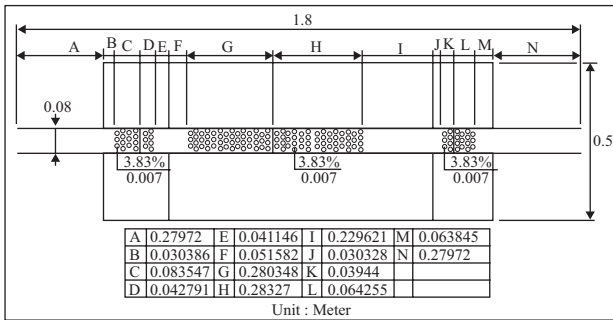
2. Discussion

To achieve a sufficient optimization, the selection of the appropriate GA parameters set is essential. As indicated in Tables 2, 4, and 6, the best GA sets with respect to three kinds of mufflers (a one-chamber, two-chamber, and a three-chamber) at the targeted pure tone noise of 250 Hz have been shown. Using the appropriate GA sets with three kinds of mufflers at the targeted pure tones (250, 550, 750 Hz), the related optimal STL curves are plotted in Figs. 8, 19, and 23. The Figs. 8, 19, and 23 reveal the predicted maximal values of the STL are precisely located at the desired frequency. Therefore, the usage of the GA optimization in finding a better design solution is reliable; moreover, all the pressure drops calculated in various mufflers can meet the specified allowable back pressure of 800 (Pa). As described in Section VI.1.1.A, in seeking a better STL with a Δp below the allowable maximal pressure drop, the compromise between parameters (Aff_{13}, Aff_{14}, Aff_{15})

Table 8. Minimization of SWL$_T$ for a broadband noise by three kinds of plug mufflers (with Δp constraint).

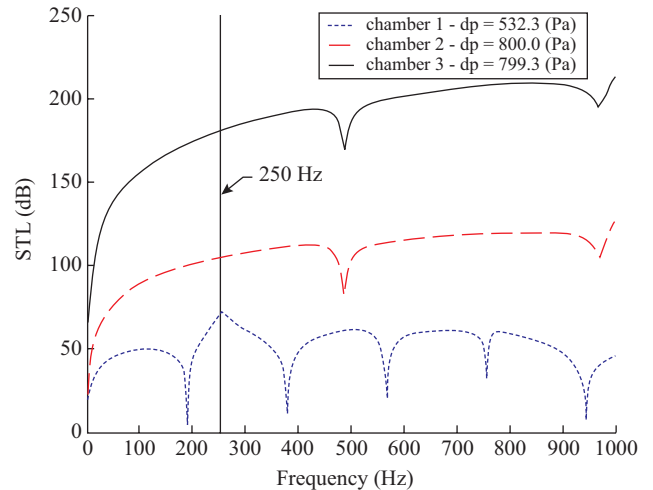| Category	Optimal GA parameters					Optimal Results				
One-chamber	*pop*	*bit*	*pm*	*pc*	*iter*$_{max}$	Aff_{11}	Aff_{12}	Aff_{13}	Aff_{14}	SWL$_T$ (dB)
						0.548	0.319	0.507	0.509	96.2
	80	10	0.05	0.6	200	$Aff15$	η$_1$	dh_1 (m)		Δp (Pa)
						0.416	0.031	0.0045		477.1
Two-chamber	*pop*	*bit*	*pm*	*pc*	*iter*$_{max}$	Aff_{21}	Aff_{22}	Aff_{23}	Aff_{24}	SWL$_T$ (dB)
						0.575	0.309	0.570	0.614	53.0
						Aff_{25}	Aff_{26}	Aff_{27}	Aff_{28}	Δp (Pa)
	80	25	0.05	0.6	500	0.571	0.524	0.575	0.858	754.3
						Aff_{29}	η$_1$	dh_1 (m)		
						0.125	0.032	0.0035		
Three-chamber	*pop*	*bit*	*pm*	*pc*	*iter*$_{max}$	Aff_{31}	Aff_{32}	Aff_{33}	Aff_{34}	SWL$_T$ (dB)
						0.689	0.681	0.576	0.393	11.9
						Aff_{35}	Aff_{36}	Aff_{37}	Aff_{38}	Δp (Pa)
						0.353	0.733	0.5098	0.845	581.9
	60	15	0.05	0.6	1000	Aff_{39}	Aff_{40}	Aff_{41}	Aff_{42}	
						0.552	0.565	0.5016	0.159	
						η$_1$	dh_1 (m)			
						0.038	0.007			
Notes: One-chamber	Aff_{11} = Lz/Lo; Aff_{12} = Lz1A/Lz; Aff_{13} = Lc1A; Aff_{14} = Lc1B/Lz1B; Aff_{15} = d1/Do									
Notes: Two-chamber	Aff_{21} = Lz/Lo; Aff_{22} = Lz1/Lz; Aff_{23} = Lz1A/Lz1; Aff_{24} = Lz2A/Lz2; Aff_{25} = Lc1A/Lz1A; Aff_{26} = Lc1B/Lz1B; Aff_{27} = Lc2A/Lz2A; Aff_{28} = Lc2B/Lz2B; Aff_{29} = d1/Do									
Notes: Three-chamber	Aff_{31} = Lz/Lo; Aff_{32} = Lz2/Lz; Aff_{33} = Lz1A/Lz1; $Aff3_4$ = Lz2A/Lz2; Aff_{35} = Lz3A/Lz3; Aff_{36} = Lc1A/Lz1A; Aff_{37} = Lc1B/Lz1B; Aff_{38} = Lc2A/Lz2A; Aff_{39} = Lc2B/Lz2B; Aff_{40} = Lc3A/Lz3A; Aff_{41} = Lc3B/Lz3B; Aff_{42} = d1/Do									

Fig. 30. Optimal shape of a three-chamber plug muffler [broadband frequency].

Fig. 31. Comparison of the STL with respect to various chambers [targeted frequency: 250 Hz].

during the numerical optimization process is obligatory.

To appreciate the acoustical effect with respect to three kinds of chambers for various tones (250, 550, 750 Hz), the STL curves have been plotted and illustrated in Figs. 31-33. As indicated in Figs. 31-33, the muffler with the most chambers has a higher acoustical performance.

Additionally, in dealing with the broadband noise using three kinds of multi-chamber plug mufflers, the GA's solution shown in Table 8 and Fig. 27 can also provide the appropriate and sufficient sound reduction under space-constraint and Δp-constrained conditions; moreover, as indicated in Fig. 27, the muffler with the most chambers can offer a higher acous-

tical performance. As can be observed in Table 8, the overall sound transmission loss with respect to three kinds of mufflers reaches 40 dB, 83.0 dB, and 124 dB.

VII. CONCLUSION

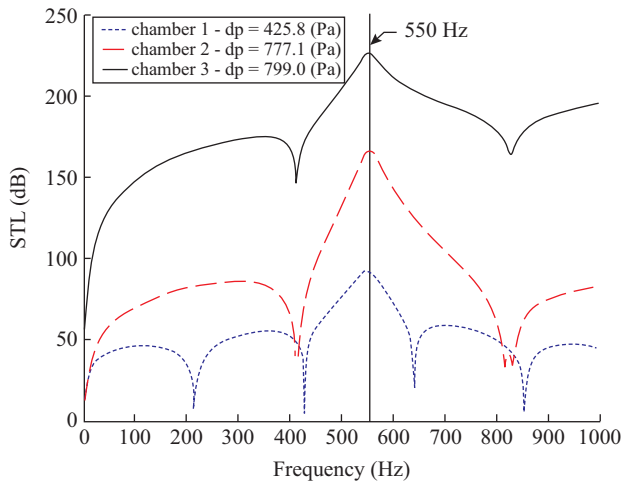It has been shown that multi-chamber plug mufflers in

Fig. 32. Comparison of the STL with respect to various chambers [targeted frequency: 550 Hz].
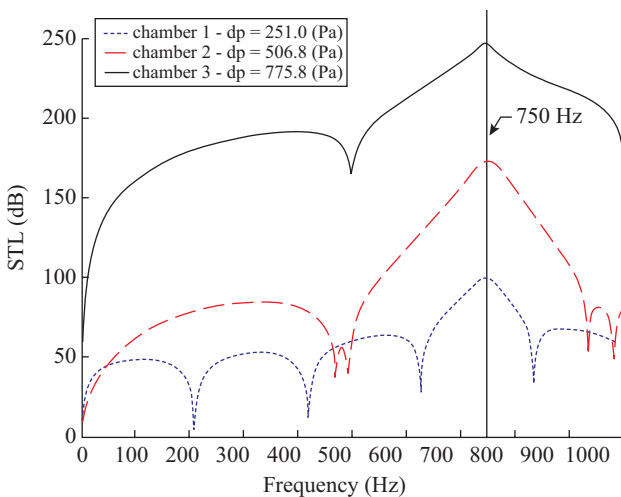

Fig. 33. Comparison of the STL with respect to various chambers [targeted frequency: 750 Hz].

conjunction with a GA optimizer can be easily and efficiently optimized under space and Δp limits by using a generalized decoupling technique, plane wave theory, as well as a four-pole transfer matrix. Five kinds of GA parameters (*pop*, *iter*$_{max}$, *bit*, *pc*, *pm*) play essential roles in the solution's accuracy during GA optimization. As indicated in Figs. 8, 19, and 23, the tuning ability established by adjusting the design parameters (the lengths of perforated and non-perforated plug ducts) of three kinds of mufflers is reliable. Moreover, the figures reveal that the noise reduction in the higher targeted frequency will be easier than that in the lower one.

To appreciate the relationships between the STL, Δp, and the design parameters, a one-chamber plug muffler has been investigated. It was found that the back pressure Δp will decrease noticeably when either the length of the chamber (Aff_{11}), the lengths of the perforated ducts (Aff_{13}, Aff_{14}), the diameter of

the inner duct (Aff_{15}), or the porosity of the inner duct (η_1) is increased; however, some of the parameters, such as the expansion ratio ($Aff_{15} = d1/Do$), were in conflict with respect to the STL and Δp. The lower the diameter of the inner duct (d1) the more visible the increment of the STL and Δp. Therefore, the compromise of Aff_{15} in simultaneously obtaining a larger STL and an acceptable (smaller) Δp during the numerical optimization is necessary.

In addition, the appropriate acoustical performance curve for three kinds of multi-chamber mufflers in depressing overall broadband noise has been assessed. As indicated in Table 8 and Fig. 27, the overall sound transmission loss with respect to three kinds of mufflers reaches 40 dB, 83.0 dB, and 124 dB.

As investigated in Section VI, to meet the requirement of the Δp limit, a compromise between the STL and Δp is compulsory during GA optimization. Under a specified Δp limit, a three-chamber muffler hybridized with a perforated plug duct exhibits an acoustical ability beyond other one-chamber mufflers and two-chamber mufflers that have been hybridized with perforated plug tubes. Beyond a doubt, the muffler with the most chambers will exhibit a better acoustical performance.

Consequently, the approach used for the optimal design of the *STL* proposed in this study within a constrained space and a back-pressure limit is indeed easy and quite effective.

ACKNOWLEDGMENTS

REFERENCES

1. Alley, B. C., Dufresne, R. M., Kanji, N., and Reesal, M. R., "Costs of workers' compensation claims for hearing Loss," *Journal of Occupational Medicine*, Vol. 31, pp. 134-138 (1989).

2. Chang, Y. C. and Chiu, M. C., "Shape optimization of one-chamber cross-flow mufflers by GA optimization," *Journal of Mechanics*, Vol. 24, pp. 13-29 (2008).

3. Chang, Y. C. and Chiu, M. C., "Shape optimization of one-chamber perforated plug/non-plug mufflers by simulated annealing method," *International Journal for Numerical Methods in Engineering*, Vol. 74, pp. 1592-1620 (2008).

4. Chiu, M. C., "Shape optimization of double-chamber side mufflers with extended tube by using four-pole matrix and simulated annealing method," *Journal of Mechanics*, Vol. 24, pp. 31-43 (2008).

5. Chiu, M. C. and Chang, Y. C., "Numerical studies on venting system with multi-chamber perforated mufflers by GA optimization," *Applied Acoustics*, Vol. 69, No. 11, pp. 1017-1037 (2008).

6. Holland, J., *Adaptation in Natural and Artificial System*, University of Michigan Press, Ann Arbor, MI (1975).

7. Jayaraman, K. and Yam, K., "Decoupling approach to modeling perforated tube muffler components," *Journal of the Acoustical Society of America*, Vol. 69, No. 2, pp. 390-396 (1981).

8. Jong, D., *An Analysis of the Behavior of a Class of Genetic Adaptive Systems*, Doctoral Thesis, Department of Computer and Communication Sciences, University of Michigan, Ann Arbor, MI (1975).

9. Kaiser, L. and Bernhardt, H., "Noise control on computer and business equipment using speed control blowers," *Proceedings of CompEuro '89., 'VLSI and Computer Peripherals. VLSI and Microelectronic Applica-*

tions in Intelligent Peripherals and their Interconnection Networks', pp. 2/114-2/117 (1989).

10. Magrab, E. B., *Environmental Noise Control*, John Wiley & Sons, New York (1975).

11. Munjal, M. L., *Acoustics of Ducts and Mufflers with Application to Exhaust and Ventilation System Design,* John Wiley & Sons, New York (1987).

12. Munjal, M. L., Krishnan, K., and Reddy, M. M., "Flow-acoustic perforated element mufflers with application to design," *Noise Control Engineering Journal*, Vol. 40, No. 1, pp. 159-167 (1993).

13. Munjal, M. L., Rao, K. N., and Sahasrabudhe, A. D., "Aeroacoustic analysis of perforated muffler components," *Journal of Sound and Vibration*, Vol. 114, No. 2, pp. 173-188. (1987).

14. Peat. K. S., "A numerical decoupling analysis of perforated pipe silencer elements," *Journal of Sound and Vibration*, Vol. 123, No. 2, pp. 199-212 (1988).

15. Sullivan, J. W., "A method of modeling perforated tube muffler components I: theory," *Journal of the Acoustical Society of America,* Vol. 66, pp. 772-778 (1979).

16. Sullivan, J. W., "A method of modeling perforated tube muffler components I: theory," *Journal of the Acoustical Society of America,* Vol. 66, pp. 779-788 (1979).

17. Sullivan, J. W. and Crocker, M. J., "Analysis of concentric tube resonators having unpartitioned cavities," *Journal of the Acoustical Society of America,* Vol. 64, pp. 207-215 (1978).

18. Thawani, P. T. and Jayaraman, K., "Modeling and applications of straight-through resonators," *Journal of the Acoustical Society of America,* Vol. 73, No. 4, pp. 1387-1389 (1983).

19. Yeh, L. J., Chang, Y. C., and Chiu, M. C., "Application of genetic algorithm to the shape optimization of a constrained double-chamber muffler with extended tubes," *Journal of Marine Science and Technology*, Vol. 12, No. 3, pp. 189-199 (2004).

20. Yeh, L. J., Chang, Y. C., Chiu, M. C., and Lai, G. J., "Computer-aided optimal design of a single-chamber muffler with side inlet/outlet under space constraints," *Journal of Marine Science and Technology*, Vol. 11, No. 4, pp. 189-196 (2003).